International Journal of Heat and Mass Transfer 52 (2009) 1928–1937

Contents lists available at ScienceDirect

International Journal of Heat and Mass Transfer

journal homepage: www.elsevier.com/locate/ijhmt

An iterative regularization method in simultaneously estimating the inlet temperature and heat-transfer rate in a forced-convection pipe

Yu-Ching Yang *, Wen-Lih Chen

Clean Energy Center, Department of Mechanical Engineering, Kun Shan University, Yung-Kang City, Tainan 710-03, Taiwan, Republic of China

ARTICLE INFO

Article history:
Received 9 June 2008
Received in revised form 23 October 2008
Available online 10 December 2008

Keywords:
Inverse problem
Conjugate gradient method
Inlet temperature
Heat-transfer rate
Pipe

ABSTRACT

In this study, an inverse algorithm based on the conjugate gradient method and the discrepancy principle is applied to estimate the unknown space- and time-dependent inlet temperature and heat-transfer rate on the external wall of a pipe system using temperature measurements at two different locations. It is assumed that no prior information is available on the functional form of the unknown inlet temperature and heat-transfer rate; hence the procedure is classified as the function estimation in inverse calculation. The temperature data obtained from the direct problem are used to simulate the temperature measurements. The accuracy of the inverse analysis is examined by using simulated exact and inexact temperature measurements. Results show that an excellent estimation on the space- and time-dependent inlet temperature and heat-transfer rate can be obtained for the test case considered in this study.

1. Introduction

Conjugate heat transfer, in which interaction occurs between the conduction effects in a solid wall and the convection effects within a fluid flowing around it, occurs in many engineering devices. The flow over fins is one of good examples involving conjugate heat transfer. In this case, accurate heat transfer characteristics can only be obtained by simultaneously analyzing the conduction in the fins and the convection in the fluid. Another example is that of a heat exchanger, in which an interaction takes place between the conduction in the pipe wall and the convection in the fluid flowing over the wall. Still there are many other examples in a variety of industries such as the cooling rods in a nuclear reactor in a nuclear power plant. Due to the significance of their role in industries, the problems associated with conjugate heat transfer have been studied by numerous researchers [1–4]. Among these problems, a particular interesting phenomenon in a pipe flow is that a substantial amount of heat can be transferred to the fluid in the unheated sections of the pipe as a result of wall conduction effects. These effects are more pronounced when the solid-to-fluid thermal conductivity ratio, k_{sf}, is high and the inner-wall radius ratio, $R_{iw} = r_{iw}/r_{ow}$, is low. In this situation, the thermal boundary conditions existing at the internal surface are not known, and hence, the energy equations must be solved with boundary conditions of both temperature and heat flux.

In recent years, the studies of inverse heat conduction problem (IHCP) have offered methods, which largely scale down experimental work, to obtain accurate thermal quantities such as heat sources, material's thermal properties, and boundary temperature or heat flux distributions, in many heat conduction problems [5–11]. While there have been many reports on IHCP, there are relatively fewer studies on inverse problems involving conjugate heat transfer, presumably due to the complex nature of the latter. Chen et al. [12] applied a technique which combined the function specification method, the whole domain estimation approach, and the linear least-squares-error method to estimate the unknown outer-wall heat flux and the inlet temperature simultaneously for conjugate heat transfer within a hydrodynamically developed turbulent pipe flow. Yet, the unknowns in Chen's study were only time-dependent functions. Zueco and Alhama [13] recently proposed a new inverse procedure to estimate the temperature-dependent thermal properties for conjugate heat transfer within a fully-developed flow in a circular pipe. In this study, a pipe system similar to [13] is considered. The space- and time-dependent fluid inlet temperature and heat-transfer rate on the pipe's external wall are simultaneously estimated by inverse method. The system includes a fully developed pipe flow, solid pipe wall, and the heat flux applied on the pipe's external wall, thus the current problem is an inverse conjugate heat transfer problem.

There are several approaches to solve an inverse problem. In this article, we present the conjugate gradient method (CGM) [14–20] and the discrepancy principle [21] to simultaneously estimate the space- and time-dependent fluid inlet temperature and heat-transfer rate on the pipe's external wall by using the simulated temperature measurements. Subsequently, the distributions of temperature in the pipe can be determined as well. The CGM belongs to a class of iterative regularization techniques, which mean the regularization procedure is performed during the iterative processes and thus the determination of optimal regularization

* Corresponding author.
E-mail address: ycyang@mail.ksu.edu.tw (Y.-C. Yang).

0017-9310/$ - see front matter © 2008 Elsevier Ltd. All rights reserved.
doi:10.1016/j.ijheatmasstransfer.2008.11.001

Nomenclature

D_1, D_2	length parameters (m)
E	thickness of the wall (m)
F	inlet temperature (K)
J	functional
J'	gradient of functional
K	thermal conductivity (W m^{-1} K^{-1})
L	length of the duct (m)
M, N	total number of measuring positions
p	direction of descent
q	heat-transfer rate at the wall (W m^{-2})
r	inner radius of the duct (m)
r	spatial radial coordinate (m)
T	temperature (K)
T_0	initial temperature (K)
t	time (sec)
u_x	axial fluid velocity (m s^{-1})
x	spatial axial coordinate (m)
Y	measurement temperature (K)
Δ	small variation quantity
α	thermal diffusivity (m^2 s^{-1})
β	step size
γ	conjugate coefficient
η	very small value
λ, φ	variable used in adjoint problem
σ	standard deviation
τ	transformed time (sec)
ϖ	random variable
Superscript	
K	iterative number
Subscripts	
f	fluid
s	solid

conditions is not needed. The conjugate gradient method is derived based on the perturbation principles and transforms the inverse problem into the solutions of three problems, namely, the direct, the sensitivity, and the adjoint problems, which will be discussed in detail in the following sections. On the other hand, the discrepancy principle is used to terminate the iteration process in the conjugate gradient method.

2. Analysis

2.1. Direct problem

To illustrate the methodology for developing expressions for use in simultaneously determining the unknown space- and time-dependent fluid inlet temperature $F(r, t)$ and heat-transfer rate $q(x, t)$ on the external wall of a fully developed pipe flow, the following transient conjugate heat transfer problem is considered. Fig. 1 shows the geometry of a fully developed pipe flow. The pipe is of length L, radius R and thickness E, and the system's initial temperature (including pipe and fluid) is T_0. Assume at time $t = 0$, the fluid inlet temperature $T_f(0,r,t)$ commences to vary as a function of space and time in the form $F(r,t)$, and the heat also starts to impose on the external surface of the pipe over the region $D_1 < x < D_2$ with a heat-transfer rate of $q(x,t)$, while the rest of the pipe's external wall is under adiabatic condition. The heat then conducts inside the solid material of the pipe towards the pipe's inner wall where the heat is transferred to the cold fluid by conjugate heat transfer. It is eventually carried downstream by the forced convection of the cold fluid flow inside the pipe. In the present simulations, the calculations of these two distributions $F(r,t)$ and $q(x,t)$ are performed simultaneously. The mathematical formulation of this transient heat transfer problem, covering the solid and fluid domains, can be expressed as [13]:

$$\frac{\partial^2 T_f}{\partial r^2}+\frac{1}{r}\frac{\partial T_f}{\partial r}+\frac{\partial^2 T_f}{\partial x^2}=u_x(r)\frac{1}{\alpha_f}\frac{\partial T_f}{\partial x}+\frac{1}{\alpha_f}\frac{\partial T_f}{\partial t}, \tag{1}$$

$$\frac{\partial^2 T_s}{\partial r^2}+\frac{1}{r}\frac{\partial T_s}{\partial r}+\frac{\partial^2 T_s}{\partial x^2}=\frac{1}{\alpha_s}\frac{\partial T_s}{\partial t}, \tag{2}$$

$$T_f = F(r,t), \quad \text{at } x = 0, \tag{3}$$

$$\frac{\partial T_s}{\partial x}=0, \quad \text{at } x = 0, \tag{4}$$

$$\frac{\partial T_s}{\partial x}=\frac{\partial T_f}{\partial x}=0, \quad \text{at } x = L, \quad 0 < r < R+E, \tag{5}$$

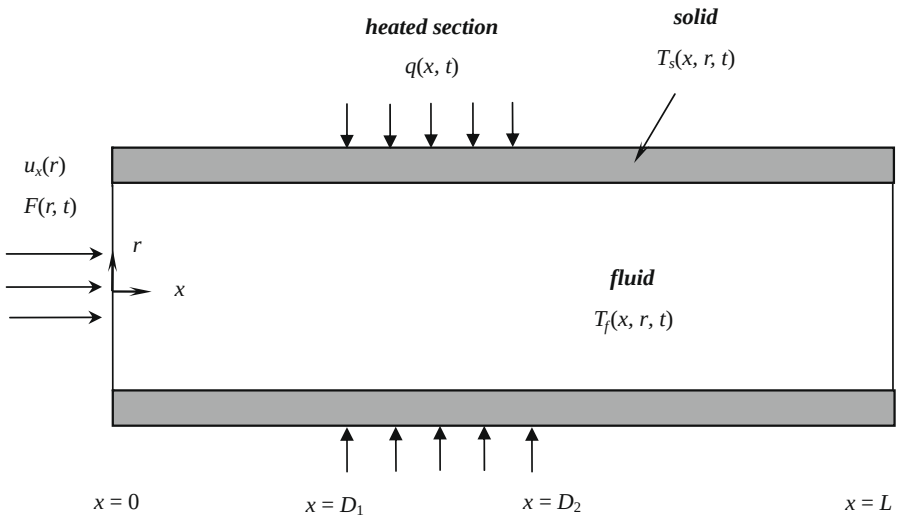

Fig. 1. Schematic of a cylindrical configuration of the pipe system.

$$\frac{\partial T_f}{\partial r}=0,\quad \text{at } r=0,\ 0<x<L, \tag{6}$$

$$T_s=T_f,\quad \text{at } r=R,\quad 0<x<L, \tag{7}$$

$$k_s\frac{\partial T_s}{\partial r}=k_f\frac{\partial T_f}{\partial r},\quad \text{at } r=R,\ 0<x<L, \tag{8}$$

$$k_s\frac{\partial T_s}{\partial r}=q(x,t),\quad \text{at } r=R+E,\ D_1<x<D_2, \tag{9}$$

$$\frac{\partial T_s}{\partial r}=0,\quad \text{at } r=R+E,\ 0<x<D_1,\ D_2<x<L, \tag{10}$$

$$T_f=T_s=T_0,\quad \text{at } t=0, \tag{11}$$

where $F(r,t)$ is the fluid inlet temperature, $q(x,t)$ is the heat-transfer rate applied along $r=R+E$ and $D_1<x<D_2$, k is the thermal conductivity, while $u_x(r)=2u_{av}[1-(r/R)^2]$ with u_{av} being the average velocity. Here the subscript s and f refer to the solid region and the fluid region, respectively. The direct problem considered here is concerned with the determination of the medium temperature when the inlet temperature $F(r,t)$, heat-transfer rate $q(x,t)$, thermal properties, and initial and boundary conditions are known.

2.2. Inverse problem

For the inverse problem, the fluid inlet temperature $F(r,t)$ and heat-transfer rate $q(x,t)$ are regarded as being unknown, while everything else in Eqs. (1)–(11) is known. In addition, temperature readings taken along the r axis at $x=x_m$ and along the x axis at $r=r_m$ are considered available. The objective of the inverse analysis is to predict the unknown space- and time-dependent $F(r,t)$ and $q(x,t)$ simultaneously from the knowledge of these temperature readings. Let the measured temperatures along the r axis at $x=x_m$ and along the x axis at $r=r_m$ be denoted by $Y_1(x_m,r,t)$ and $Y_2(x,r_m,t)$, respectively. Then this inverse problem can be stated as follows: by utilizing the above mentioned measured temperature data $Y_1(x_m,r,t)$ and $Y_2(x,r_m,t)$, the unknowns $F(r,t)$ and $q(x,t)$ are to be estimated simultaneously over the specified domain.

The solution of the present inverse problem is to be obtained in such a way that the following functional is minimized:

$$J[F(r,t),q(x,t)]=\int_{t=0}^{t_f}\sum_{i=1}^{M}\left[T_f(x_m,r_i,t)-Y_1(x_m,r_i,t)\right]^2\mathrm{d}t + \int_{t=0}^{t_f}\sum_{j=1}^{N}\left[T_s(x_j,r_m,t)-Y_2(x_j,r_m,t)\right]^2\mathrm{d}t, \tag{12}$$

here M and N are the total numbers of measuring positions along the r axis of $x=x_m$ and along the x axis of $r=r_m$, respectively, while $T_f(x_m,r_i,t)$ and $T_s(x_j,r_m,t)$ are the estimated (or computed) temperatures at the measurement locations. These quantities are determined from the solution of the direct problem given previously by using an estimated $\tilde{F}^K(r,t)$ and $\tilde{q}^K(x,t)$ for the exact $F(r,t)$ and $q(x,t)$, respectively. Here $\tilde{F}^K(r,t)$ and $\tilde{q}^K(x,t)$ denote the estimated quantities at the Kth iteration. t_f is the final time of the measurement. In addition, in order to develop expressions for the determination of the unknowns $F(r,t)$ and $q(x,t)$, a "sensitivity problem" and an "adjoint problem" are constructed as described below.

2.3. Sensitivity problem

Since the problem involves two unknowns, the fluid inlet temperature $F(r,t)$ and heat-transfer rate $q(x,t)$, and in order to derive the sensitivity problem for each unknown, we should perturb the unknown function one at a time. It is assumed that when $F(r,t)$ undergoes a variation $\Delta F(r,t)$, $T_f(x,r,t)$ and $T_s(x,r,t)$ are perturbed by $T_f+\Delta T_{f1}$ and $T_s+\Delta T_{s1}$, respectively. Then replacing in the direct problem F by $F+\Delta F$, T_f by $T_f+\Delta T_{f1}$ and T_s by $T_s+\Delta T_{s1}$, subtracting from the resulting expressions the direct problem, and neglecting the second-order terms, the following sensitivity problem for the sensitivity function ΔT_{f1} and ΔT_{s1} can be obtained.

$$\frac{\partial^2\Delta T_{f1}}{\partial r^2}+\frac{1}{r}\frac{\partial\Delta T_{f1}}{\partial r}+\frac{\partial^2\Delta T_{f1}}{\partial x^2}=u_x\frac{1}{\alpha_f}\frac{\partial\Delta T_{f1}}{\partial x}+\frac{1}{\alpha_f}\frac{\partial\Delta T_{f1}}{\partial t}, \tag{13}$$

$$\frac{\partial^2\Delta T_{s1}}{\partial r^2}+\frac{1}{r}\frac{\partial\Delta T_{s1}}{\partial r}+\frac{\partial^2\Delta T_{s1}}{\partial x^2}=\frac{1}{\alpha_s}\frac{\partial\Delta T_{s1}}{\partial t}, \tag{14}$$

$$\Delta T_{f1}=\Delta F(r,t),\quad \text{at } x=0, \tag{15}$$

$$\frac{\partial\Delta T_{s1}}{\partial x}=0,\quad \text{at } x=0, \tag{16}$$

$$\frac{\partial\Delta T_{s1}}{\partial x}=\frac{\partial\Delta T_{f1}}{\partial x}=0,\quad \text{at } x=L,\ 0<r<R+E, \tag{17}$$

$$\frac{\partial\Delta T_{f1}}{\partial r}=0,\quad \text{at } r=0,\ 0<x<L, \tag{18}$$

$$\Delta T_{s1}=\Delta T_{f1},\quad \text{at } r=R,\ 0<x<L, \tag{19}$$

$$k_s\frac{\partial\Delta T_{s1}}{\partial r}=k_f\frac{\partial\Delta T_{f1}}{\partial r},\quad \text{at } r=R,\ 0<x<L, \tag{20}$$

$$k_s\frac{\partial\Delta T_{s1}}{\partial r}=0,\quad \text{at } r=R+E,\ D_1<x<D_2, \tag{21}$$

$$\frac{\partial\Delta T_{s1}}{\partial r}=0,\quad \text{at } r=R+E,\ 0<x<D_1,\ D_2<x<L, \tag{22}$$

$$\Delta T_{f1}=\Delta T_{s1}=0,\quad \text{at } t=0. \tag{23}$$

The sensitivity problem of Eqs. (13)–(23) can be solved by the same method as the direct problem of Eqs. (1)–(11). Similarly, by perturbing $q(x,t)$ with $\Delta q(x,t)$, the second sensitivity problem for the sensitivity functions ΔT_{f2} and ΔT_{s2} can be obtained.

2.4. Adjoint problem and gradient equation

To obtain the adjoint problem, Eqs. (1) and (2) are multiplied by the Lagrange multipliers (or adjoint functions) $\lambda_s(x,r,t)$ and $\lambda_f(x,r,t)$, respectively, and the resulting expressions are integrated over the time and correspondent space domains. Then the results are added to the right hand side of Eq. (12) to yield the following expression for the functional $J[F(r,t),q(x,t)]$:

$$\begin{aligned}J[F(r,t),q(x,t)]=&\int_{t=0}^{t_f}\sum_{i=1}^{M}[T_f(x_m,r_i,t)-Y_1(x_m,r_i,t)]^2\,\mathrm{d}t\\&+\int_{t=0}^{t_f}\sum_{j=1}^{N}[T_s(x_j,r_m,t)-Y_2(x_j,r_m,t)]^2\,\mathrm{d}t\\&+\int_0^{t_f}\int_{r=0}^{R}\int_{x=0}^{L}r\cdot\lambda_f\cdot\left[\frac{\partial^2T_f}{\partial r^2}+\frac{1}{r}\frac{\partial T_f}{\partial r}+\frac{\partial^2T_f}{\partial x^2}\right.\\&\left.-u_x\frac{1}{\alpha_f}\frac{\partial T_f}{\partial x}-\frac{1}{\alpha_f}\frac{\partial T_f}{\partial t}\right]\mathrm{d}x\,\mathrm{d}r\,\mathrm{d}t+\int_0^{t_f}\int_{r=R}^{R+E}\int_{x=0}^{L}r\cdot\lambda_s\\&\cdot\left[\frac{\partial^2T_s}{\partial r^2}+\frac{1}{r}\frac{\partial T_s}{\partial r}+\frac{\partial^2T_s}{\partial x^2}-\frac{1}{\alpha_s}\frac{\partial T_s}{\partial t}\right]\mathrm{d}x\,\mathrm{d}r\,\mathrm{d}t.\end{aligned} \tag{24}$$

The variation ΔJ_1 is obtained by perturbing $F(r,t)$ by $\Delta F(r,t)$, $T_f(x,r,t)$ and $T_s(x,r,t)$ are perturbed by ΔT_{f1} and ΔT_{s1}, respectively, in Eq. (24). Subtracting from the resulting expression the original Eq. (24) and neglecting the second-order terms, we thus find

$$\Delta J_1[F(r,t),q(x,t)] = \int_0^{t_f}\int_{r=0}^{R}\int_{x=0}^{L}\sum_{i=1}^{M} 2\left[T_f(x,r,t)-Y_1(x,r,t)\right]\Delta T_{f1} \cdot \delta(r-r_i)\cdot\delta(x-x_m)\,dx\,dr\,dt + \int_0^{t_f}\int_{r=R}^{R+E}\int_{x=0}^{L}\sum_{j=1}^{N} 2[T_s(x,r,t)-Y_2(x,r,t)]\Delta T_{s1} \cdot \delta(r-r_m)\cdot\delta(x-x_j)\,dx\,dr\,dt + \int_0^{t_f}\int_{r=0}^{R}\int_{x=0}^{L} r\cdot\lambda_f \cdot\left[\frac{\partial^2\Delta T_{f1}}{\partial r^2}+\frac{1}{r}\frac{\partial\Delta T_{f1}}{\partial r}+\frac{\partial^2\Delta T_{f1}}{\partial x^2}-u_x\frac{1}{\alpha_f}\frac{\partial\Delta T_{f1}}{\partial x} -\frac{1}{\alpha_f}\frac{\partial\Delta T_{f1}}{\partial t}\right]dx\,dr\,dt + \int_0^{t_f}\int_{r=R}^{R+E}\int_{x=0}^{L} r\cdot\lambda_s \cdot\left[\frac{\partial^2\Delta T_{s1}}{\partial r^2}+\frac{1}{r}\frac{\partial\Delta T_{s1}}{\partial r}+\frac{\partial^2\Delta T_{s1}}{\partial x^2}-\frac{1}{\alpha_s}\frac{\partial\Delta T_{s1}}{\partial t}\right]dx\,dr\,dt, \tag{25}$$

where δ is the Dirac function. We can integrate the third and fourth triple integral terms in Eq. (25) by parts. Utilizing the initial and boundary conditions of the sensitivity problem, then ΔJ_1 is allowed to go to zero. The vanishing of the integrands containing ΔT_{f1}; and ΔT_{s1} leads to the following adjoint problem for the determination of $\lambda_f(x,r,t)$ and $\lambda_s(x,r,t)$:

$$\frac{\partial^2\lambda_f}{\partial r^2}+\frac{1}{r}\frac{\partial\lambda_f}{\partial r}+\frac{\partial^2\lambda_f}{\partial x^2}+u_x\frac{1}{\alpha_f}\frac{\partial\lambda_f}{\partial x}+\frac{1}{\alpha_f}\frac{\partial\lambda_f}{\partial t} + \sum_{i=1}^{M}\frac{2[T_f(x,r,t)-Y_1(x,r,t)]}{r}\cdot\delta(x-x_m)\cdot\delta(r-r_i)=0, \tag{26}$$

$$\frac{\partial^2\lambda_s}{\partial r^2}+\frac{1}{r}\frac{\partial\lambda_s}{\partial r}+\frac{\partial^2\lambda_s}{\partial x^2}+\frac{1}{\alpha_s}\frac{\partial\lambda_s}{\partial t}+\sum_{j=1}^{N}\frac{2[T_s(x,r,t)-Y_2(x,r,t)]}{r} \cdot\delta(x-x_j)\cdot\delta(r-r_m)=0, \tag{27}$$

$$\lambda_f = 0, \quad \text{at } x=0, \tag{28}$$

$$\frac{\partial\lambda_s}{\partial x}=0, \quad \text{at } x=0, \tag{29}$$

$$\frac{\partial\lambda_f}{\partial x}+\frac{u_x}{\alpha_f}\lambda_f=0, \quad \text{at } x=L,\ 0<r<R, \tag{30}$$

$$\frac{\partial\lambda_s}{\partial x}=0, \quad \text{at } x=L,\ R<r<R+E, \tag{31}$$

$$\frac{\partial\lambda_f}{\partial r}=0, \quad \text{at } r=0,\ 0<x<L, \tag{32}$$

$$k_f\lambda_s = k_s\lambda_f, \quad \text{at } r=R,\ 0<x<L, \tag{33}$$

$$\frac{\partial\lambda_s}{\partial r}=\frac{\partial\lambda_f}{\partial r}, \quad \text{at } r=R,\ 0<x<L, \tag{34}$$

$$\frac{\partial\lambda_s}{\partial r}=0, \quad \text{at } r=R+E,\ 0<x<L, \tag{35}$$

$$\lambda_f=\lambda_s=0, \quad \text{at } t=t_f. \tag{36}$$

The adjoint problem is different from the standard initial value problem in that the final time condition at time $t = t_f$ is specified instead of customary initial condition. However, this problem can be transformed to an initial value problem by the transformation of the time variable as $\tau = t_f - t$. Then the adjoint problem can be solved by the same method as the direct problem.

Finally the following integral term is left

$$\Delta J_1(r,t) = \int_0^{t_f}\int_{r=0}^{R} r\cdot\frac{\partial\lambda_f(0,r,t)}{\partial x}\cdot\Delta F(r,t)\,dr\,dt. \tag{37}$$

From the definition used in Ref. [17], we have

$$\Delta J_1(r,t) = \int_0^{t_f}\int_{r=0}^{R} J_1'\cdot\Delta F(r,t)\,dr\,dt \tag{38}$$

where $J_1'(r,t)$ is the gradient of the functional J_1, a comparison of Eqs. (37) and (38) leads to the following form:

$$J_1'[F(r,t)] = r\cdot\frac{\partial\lambda_f(0,r,t)}{\partial x} \tag{39}$$

Similarly, Eqs. (1) and (2) are multiplied by the Lagrange multiplier (or adjoint function) $\varphi_f(x,r,t)$ and $\varphi_s(x,r,t)$ to derive the adjoint problem for the case when perturbing $\Delta q(x,t)$. Following the same procedure, eventually, we find that the solutions for adjoint equations of $\varphi_f(x,r,t)$ and $\varphi_s(x,r,t)$ are identical to those for $\lambda_f(x,r,t)$ and $\lambda_s(x,r,t)$. This implies that the adjoint equations need to be solved only once since $\lambda_f(x,r,t) = \phi_f(x,r,t)$ and $\lambda_s(x,r,t) = \phi_s(x,r,t)$. Finally the gradient equation for $q(x,t)$ can be obtained as

$$J_2'[q(x,t)] = -(R+E)\cdot\phi_s(x,R+E,t)/k_s \tag{40}$$

2.5. Conjugate gradient method for minimization

The following iteration process based on the conjugate gradient method is now used for the simultaneous estimation of $F(r,t)$ and $q(x,t)$ by minimizing the above functional $J[F(r,t),q(x,t)]$:

$$\tilde{F}^{k+1}(r,t) = \tilde{F}^{k}(r,t) - \beta_1^K p_1^K(r,t) \quad K=0,1,2,\ldots., \tag{41}$$

$$\tilde{q}^{k+1}(x,t) = \tilde{q}^{k}(x,t) - \beta_2^K p_2^K(x,t) \quad K=0,1,2,\ldots., \tag{42}$$

where β_1^K and β_2^K are the search step size in going from iteration K to iteration $K+1$, and $p_1^K(r,t)$ and $p_2^K(x,t)$ are the direction of descent (i.e., search direction) given by

$$p_1^K(r,t) = J_1'^K(r,t) + \gamma_1^K p_1^{K-1}(r,t), \tag{43}$$

$$p_2^K(x,t) = J_2'^K(x,t) + \gamma_2^K p_2^{K-1}(x,t). \tag{44}$$

The expressions for the conjugate coefficient γ_1^K and γ_2^K can be found in [17]. To perform the iteration according to Eqs. (41) and (42), we need to compute the step size β_1^K and β_2^K, and the gradient of functional $J_1'^K(r,t)$ and $J_2'^K(x,t)$. The β_1^K and β_2^K are computed by minimizing $J[\tilde{F}^{k+1}(r,t),\tilde{q}^{k+1}(x,t)]$ given by Eq. (12) with respect to β_1^K and β_2^K, respectively [22]. On the other hand, the gradient of functional $J_1'^K(r,t)$ and $J_2'^K(x,t)$ are obtained from the solutions of adjoint problem.

2.6. Stopping criterion

If the problem contains no measurement errors, the traditional check condition specified as

$$J[\tilde{F}^{k+1}(r,t),\tilde{q}^{k+1}(x,t)] < \eta \tag{45}$$

where η is a small specified number, can be used as the stopping criterion. However, the observed temperature data contains measurement errors; as a result, the inverse solution will tend to approach the perturbed input data, and the solution will exhibit oscillatory behavior as the number of iteration is increased [23]. Computational experience has shown that it is advisable to use the discrepancy principle [21] for terminating the iteration process in the conjugate gradient method. Assuming $T_f(x_m,r_i,t) - Y_1(x_m,r_i,t) \cong T_s(x_j,r_m,t) - Y_2(x_j,r_m,t) \cong \sigma$, where σ is the standard deviation of the measurement error, the stopping criteria η by the discrepancy principle can be obtained from Eq. (12) as

$$\eta = \sigma^2 t_f(M+N). \tag{46}$$

Then the stopping criterion is given by Eq. (45) with η determined from Eq. (46).

2.7. Computational procedures

The computational procedure for the solution of this inverse problem may be summarized as follows:

Suppose $\widetilde{F}^K(r,t)$ and $\tilde{q}^K(x,t)$ is available at iteration K.

Step 1 Solve the direct problem given by Eqs. (1)–(11) for $T_f(x_m, r_i, t)$ and $T_s(x_j, r_m, t)$, respectively.

Step 2 Examine the stopping criterion given by Eq. (45) with η given by Eq. (46). Continue if not satisfied.

Step 3 Solve the adjoint problem given by Eqs. (26)–(36) for $\lambda_f(x,r,t)$ and $\lambda_s(x,r,t)$, respectively.

Step 4 Compute the gradient of the functional $J_1'[F(r,t)]$ and $J_2'[q(x,t)]$ from Eqs. (39) and (40), respectively.

Step 5 Compute the conjugate coefficients γ_1^K and γ_1^K and the direction of decent $p_1^K(r,t)$ and $p_2^K(x,t)$, respectively.

Step 6 Set $\Delta F(r,t) = p_1^K$ and $\Delta q(x,t) = p_2^K$, and solve the sensitivity problem for $\Delta T_{f1}(x_m, r_i, t)$, $\Delta T_{s1}(x_j, r_m, t)$ and $\Delta T_{f2}(x_m, r_i, t)$, $\Delta T_{s2}(x_j, r_m, t)$.

Step 7 Compute the search step size β_1^K and β_2^K.

Step 8 Compute the new estimation for $\widetilde{F}^{K+1}(r,t)$ and $\tilde{q}^{K+1}(x,t)$ from Eqs. (41) and (42), and return to Step 1.

3. Results and discussion

In the present study, we assume the material of the pipe wall being steel and the fluid being air. Then the material properties and the geometric parameters of the system are listed as follows:

$$\alpha_s = 1.5\times10^{-5}\ \mathrm{m^2\ s^{-1}},\quad \alpha_f = 2.2\times10^{-5}\ \mathrm{m^2\ s^{-1}},$$
$$k_s = 52\ \mathrm{W\ m^{-1}\ K^{-1}},\ k_f = 0.0262\ \mathrm{W\ m^{-1}\ K^{-1}},\quad R = 0.2\ \mathrm{m},$$
$$E = 0.02\ \mathrm{m},\quad L = 1.5\ \mathrm{m}, D_1 = 0.4\ \mathrm{m}, D_2 = 1.1\ \mathrm{m}.$$

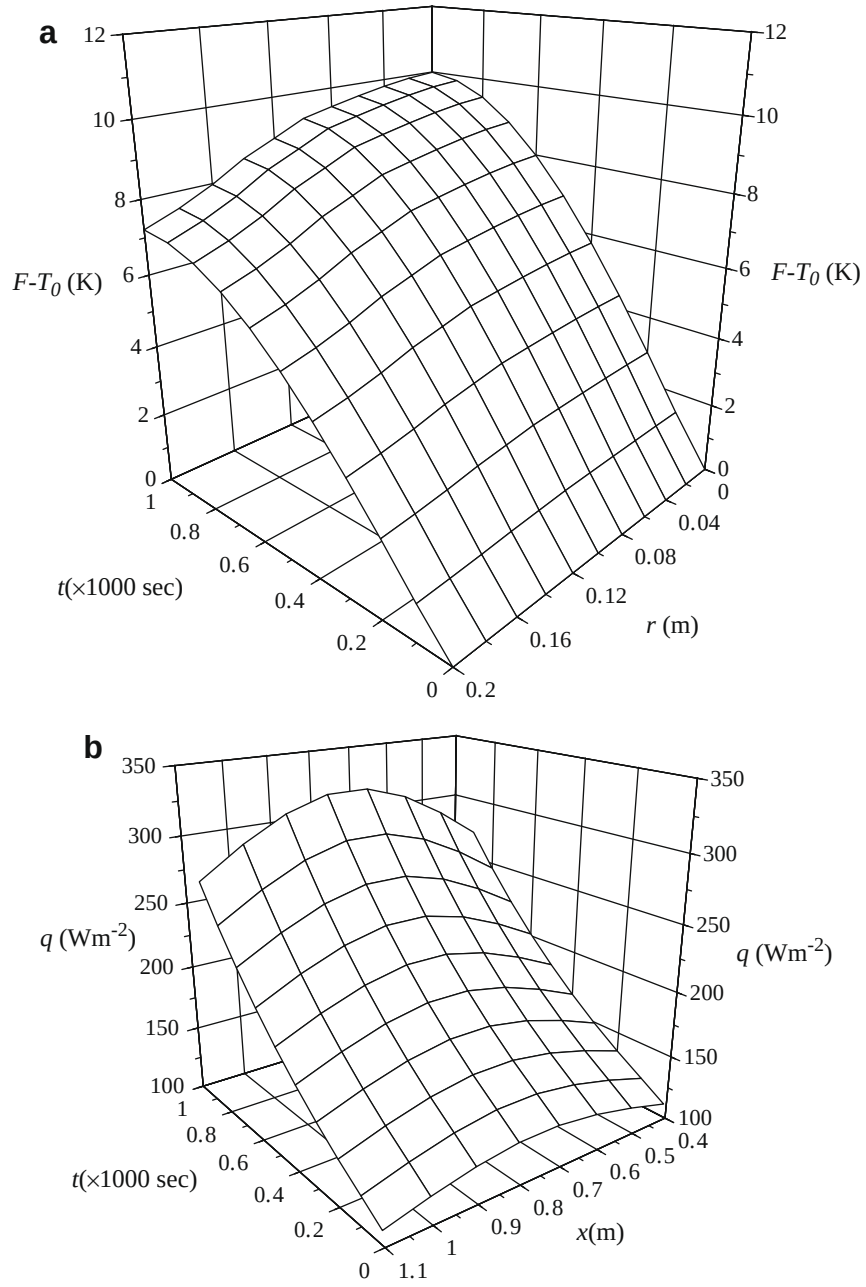

Fig. 2. Exact distributions: (a) inlet temperature $F(r,t) - T_0$ and (b) heat-transfer rate $q(x,t)$.

The flow in the pipe is assumed to be laminar and fully developed; hence the velocity profile is:

$$u_x(r) = 2u_{av}\left[1 - \left(\frac{r}{R}\right)^2\right],$$

where u_{av} is the bulk averaged velocity of the pipe flow and is set to be 0.2 m s^{-1} in this study.

The objective of this article is to validate the present approach when used to simultaneously estimate the space- and time-dependent inlet temperature $F(r,t)$ and heat-transfer rate $q(x,t)$ on a pipe's external wall accurately without prior information on the functional form of the unknown quantities, a procedure called function estimation. In order to illustrate the accuracy of the present inverse analysis, we consider the simulated exact distributions of inlet temperature and heat-transfer rate, $F(r,t)$ and $q(x,t)$ as:

$$F(r,t) = 10\cos\left(0.25\frac{r}{R}\pi\right)\sin\left(\frac{\pi t}{2000}\right)\ \mathrm{K}, \tag{47}$$

and

$$q(x,t) = \left[100 + 20\sin\left(\frac{x - D_1}{D_2 - D_1}\pi\right)\right]e^{\frac{t}{1000}}\ \mathrm{W\,m^{-2}}, \tag{48}$$

respectively. In addition, the thermocouples are located along the r axis of $x = x_m = 0.04$ m and along the x axis of $r = r_m = 0.2159$ m, respectively. The heat-transfer-rate function $q(x,t)$ is so formulated that at any moment, the quantity has its maximum value occurring

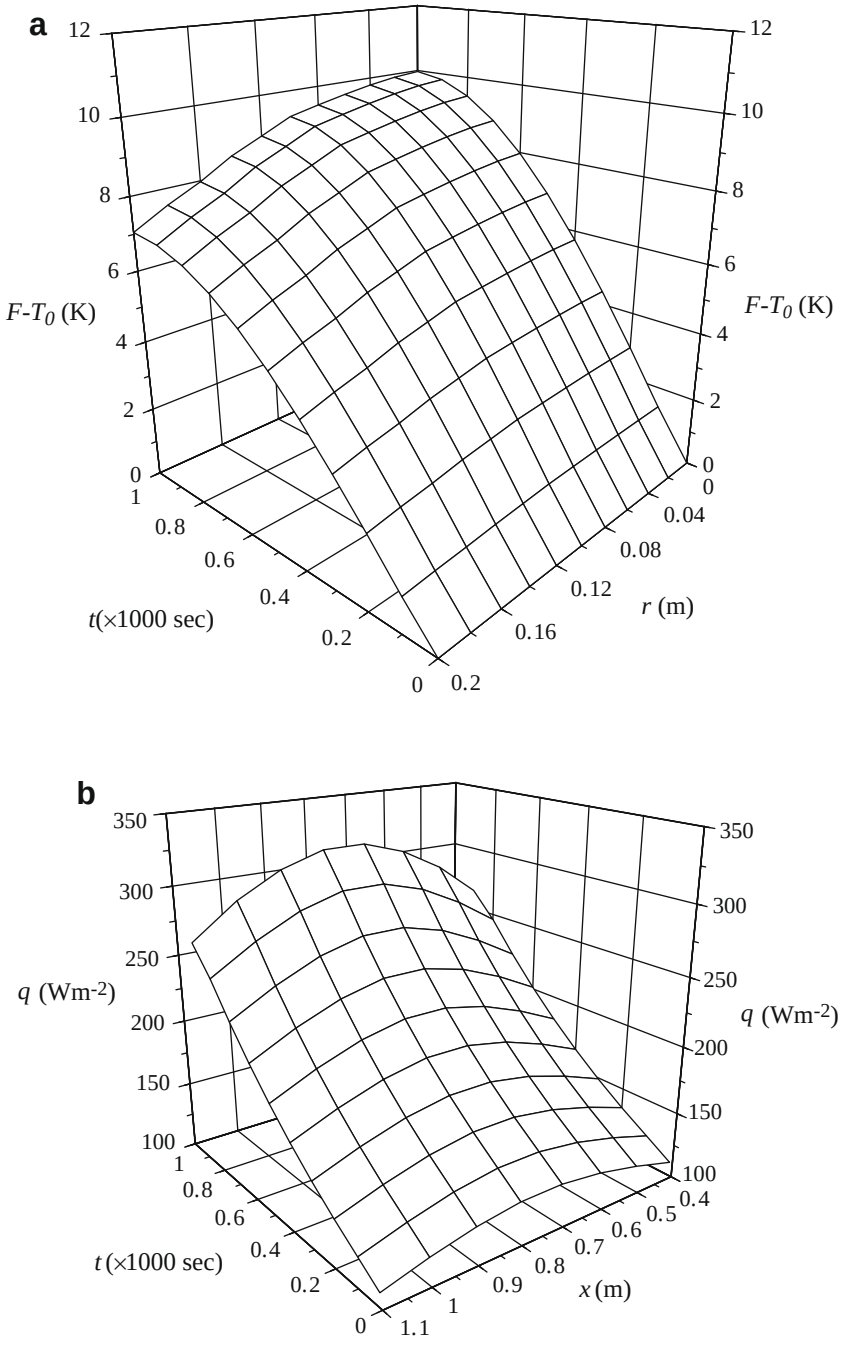

Fig. 3. Estimated distributions with $\sigma = 0.0$ and initial guesses $\tilde{F}^0 = T_0$ and $\tilde{q}^0 = 0$: (a) inlet temperature $F(r, t) - T_0$ and (b) heat-transfer rate $q(x,t)$.

at the center of the heated section and gradually reduces towards the two ends of the heated section. Additionally, the magnitude of the quantity increases in general as time elapses, simulating a gradual increase of heating power. The plots of the exact $F(r,t)$ and $q(x,t)$ are shown in Fig. 2(a) and (b), respectively. The selection of the exact heat-transfer rate is also for the purpose of demonstrating that an accurate estimation of $q(x,t)$ can be obtained using the current method despite the complexity of the functional form of $q(x,t)$ itself.

The numerical procedure in this paper is based on the unstructured-mesh, fully collocated, finite-volume code, 'USTREAM' developed by the second author. This is the descendent of the structured-mesh, multi-block code of 'STREAM' [24]. Due to the fact that the computational domain is symmetrical to the center line of the pipe, only the upper half of the domain is solved for the inverse problem. Also in the current problem, the vicinity of heated section is the most important part as far as heat transfer is concerned; hence fine mesh is used in this region. For the rest of the wall, a coarser mesh is applied. Subsequently, there are 30 and 20 cells allocated for heated section and the rest of the pipe, respectively in the axial direction. The thermocouples are assumed located at the same positions as the surface grid cells inside the heated region. Along the radial direction, on the other hand, we found that at least 5 cells are needed to obtain grid-independent solutions even for the relative thin pipe wall. Therefore, 5 and 20 cells are respectively allocated for the solid pipe wall and the fluid space inside the pipe. In terms of the temporal domain, the total measurement time is chosen as $t_f = 1000$ sec and measurement time step is taken to be 10 sec. The specification of this relative long time duration is because the thermal diffusivities for both solid and fluid materials are very small, resulting in a very slow development of thermal field in the system. Even with the duration of 1000 sec and the heat-transfer rate specified in this study, the maximum temperature is only about 3 degree higher than the initial temperature at the end of the time period.

In the analysis, we do not have a real experimental set up to measure the temperatures Y_1 and Y_2 in Eq. (12). Instead, we

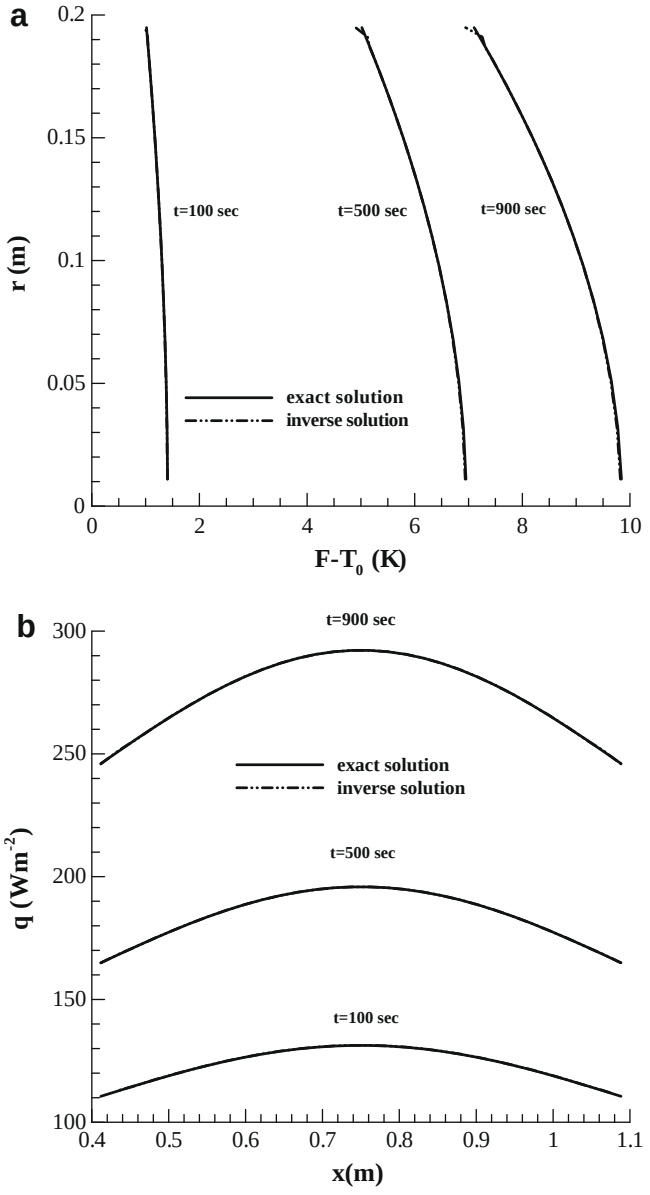

Fig. 4. Estimated distributions at $t = 100$, 500, and 900 sec, respectively, with $\sigma = 0.0$ and initial guesses $\tilde{F}^0 = T_0$ and $\tilde{q}^0 = 0$: (a) inlet temperature $F(r,t) - T_0$ and (b) heat-transfer rate $q(x,t)$.

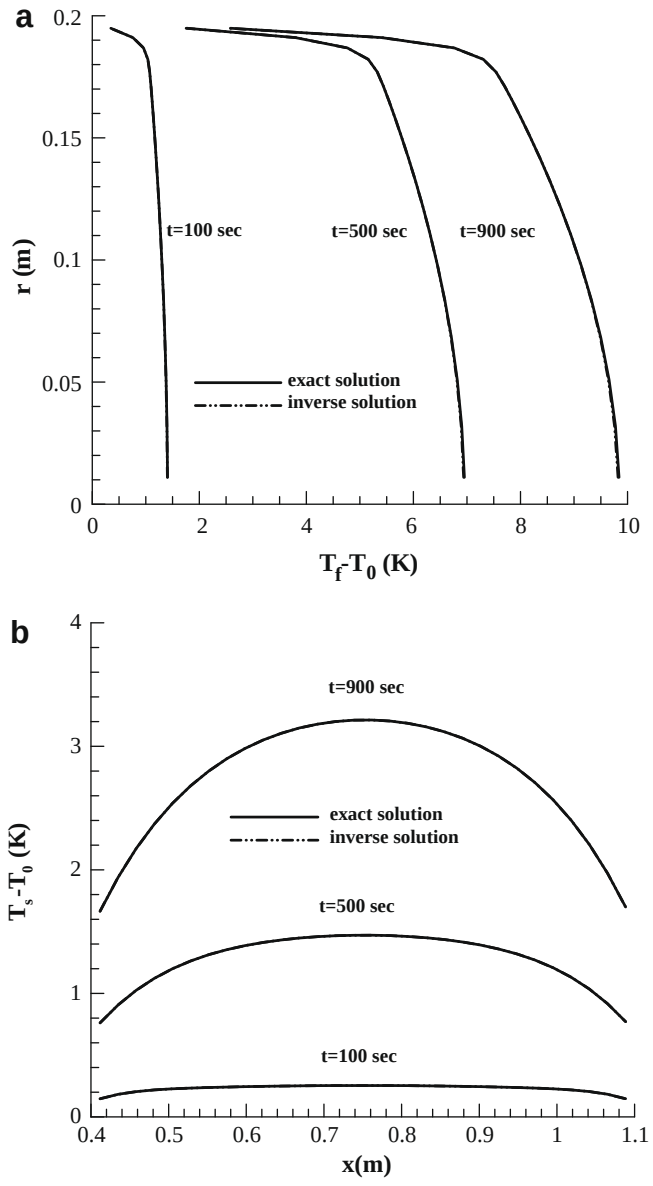

Fig. 5. Estimated temperature distributions on measurement points at $t = 100$, 500, and 900 sec, respectively, with $\sigma = 0.0$ and initial guesses $\tilde{F}^0 = T_0$ and $\tilde{q}^0 = 0$: (a) $x_m = 0.04$ m (b) $r_m = 0.2159$ m.

substitute the simulated exact $F(r,t)$ and $q(x,t)$ in Eqs. (47) and (48) into the direct problem of Eqs. (1)–(11) to calculate the temperatures at the locations where the thermocouples are placed. The results are taken as the computed temperature Y_{exact}. Meanwhile, in order to consider the situation of measurement errors, a random error noise is added to the above computed temperature Y_{exact} to obtain the measured temperaturesY_1 and Y_2. Hence, the measured temperature Y is expressed as:

$$Y = Y_{exact} + \varpi\sigma,$$

where ϖ is a random variable within −2.576 to 2.576 for a 99% confidence bounds, and σ is the standard deviation of the measurement. The measured temperatures Y_1 and Y_2 generated in such way are the so-called simulated measurement temperatures.

The inverse solutions obtained from the numerical experiments with the initial guess values $\tilde{F}^0(r,t) = \mathrm{T_0\ K}$, $\tilde{q}^0(x,t) = 0\ \mathrm{W\ m^{-2}}$, and no measurement errors ($\sigma = 0.0$) are shown in Fig. 3. The comparison between Figs. 2 and 3 shows that the estimated values for inlet temperature and heat-transfer rate are almost identical to the exact values of $F(r,t)$ and $q(x,t)$. Fig. 4 demonstrates the comparison of the estimated values for inlet temperature and heat-transfer rate with the exact values at t = 100, 500, and 900 sec, respectively, for measurement error of deviation $\sigma = 0.0$ and initial guess values $\tilde{F}^0(r,t) = T_0\ \mathrm{K}$, $\tilde{q}^0(x,t) = 0\ \mathrm{W\ m^{-2}}$. Fig. 5 depicts the estimated and exact temperature profiles on the measurement points at t = 100, 500, and 900 sec, respectively, with the same measurement error and initial guess values as those of Figs. 3 and 4. It can be found in Figs. 4 and 5 that the predicted values are in excellent agreement with the exact results.

In order to investigate the effect of measurement error on the accuracy of the estimated values, Fig. 6 illustrates the inverse solutions of $F(r,t)$ and $q(x,t)$, obtained with the measurement error of

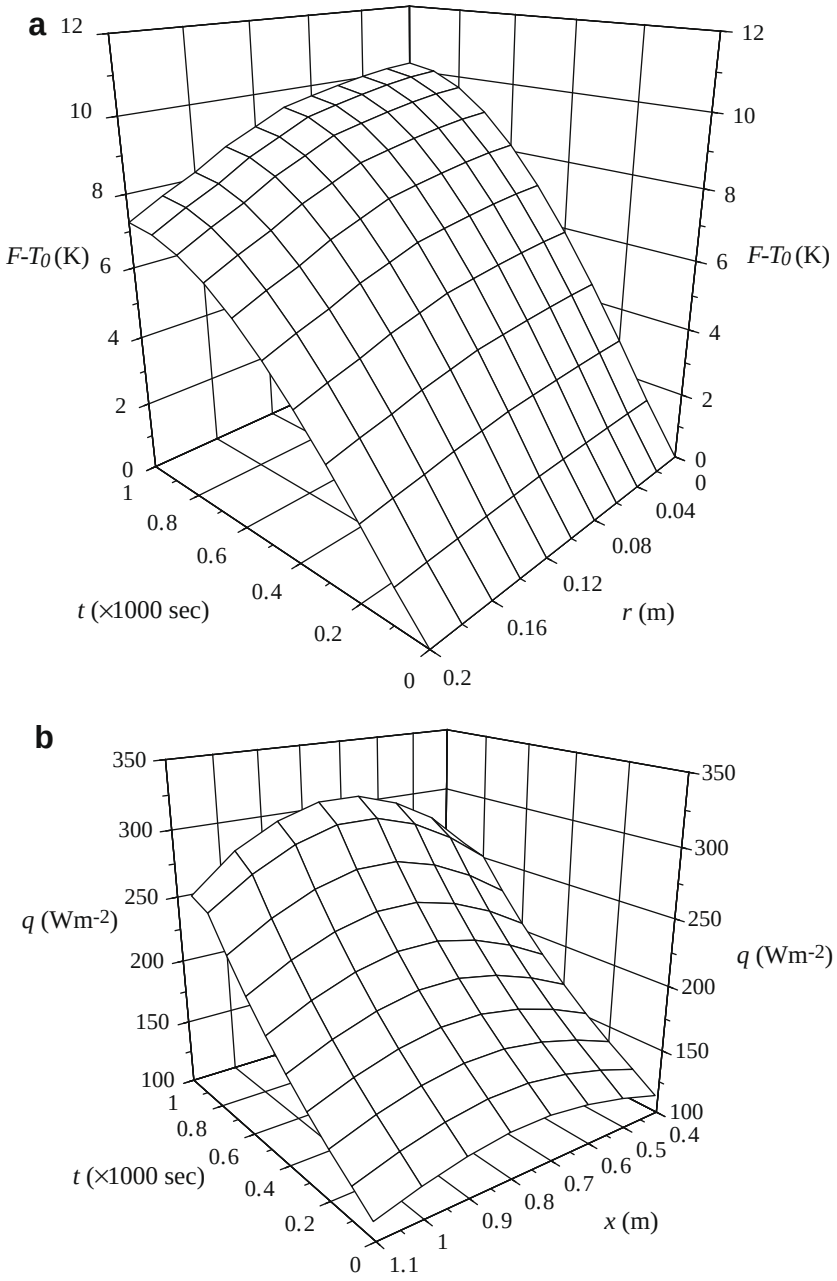

Fig. 6. Estimated distributions with $\sigma = 0.01$ and initial guesses $\tilde{F}^0 = T_0$ and $\tilde{q}^0 = 0$: (a) inlet temperature $F(r,t) - T_0$ and (b) heat-transfer rate $q(x,t)$.

deviation $\sigma = 0.01$ and initial guess values $\widetilde{F}^0(r,t) = T_0$ K, $\tilde{q}^0(x,t) = 0$ W m^{-2}. For a temperature of unity and 99% confidence, that standard deviation, $\sigma = 0.01$, corresponds to measurement error of 2.58%. A comparison among Figs. 2, 3 and 6 reveals that, for the cases considered in this study, increase in the measurement error does not cause obvious decrease on the accuracy of the inverse solution. The estimated values of $F(r,t)$ and $q(x,t)$ at $t = 100$, 500, and 900 sec, respectively, with the same measurement error and initial guess values as those of Fig. 6 are shown in Fig. 7. Figs. 6 and 7 prove that the proposed inverse method is still capable of yielding satisfactory results even when a measurement error ($\sigma = 0.01$) is introduced. Finally, with inlet temperature and heat-transfer rate been accurately estimated, the temperature distributions across the entire domain can also be accurately calculated. Fig. 8 shows the temperature distributions along the radial direction at $x = 0.75$ m at $t = 100$, 500, and 900 sec for $\sigma = 0.0$ and 0.01, respectively. The initial guess values for Fig. 8 are $\widetilde{F}^0(r,t) = 0$ K, $\tilde{q}^0(x,t) = 0$ W m^{-2}. It can be seen that the estimated temperature with $\sigma = 0.0$ is virtually identical to the exact temperature at the 3 time steps shown, while there are only minor differences between the exact temperature and the estimated temperature with $\sigma = 0.01$.

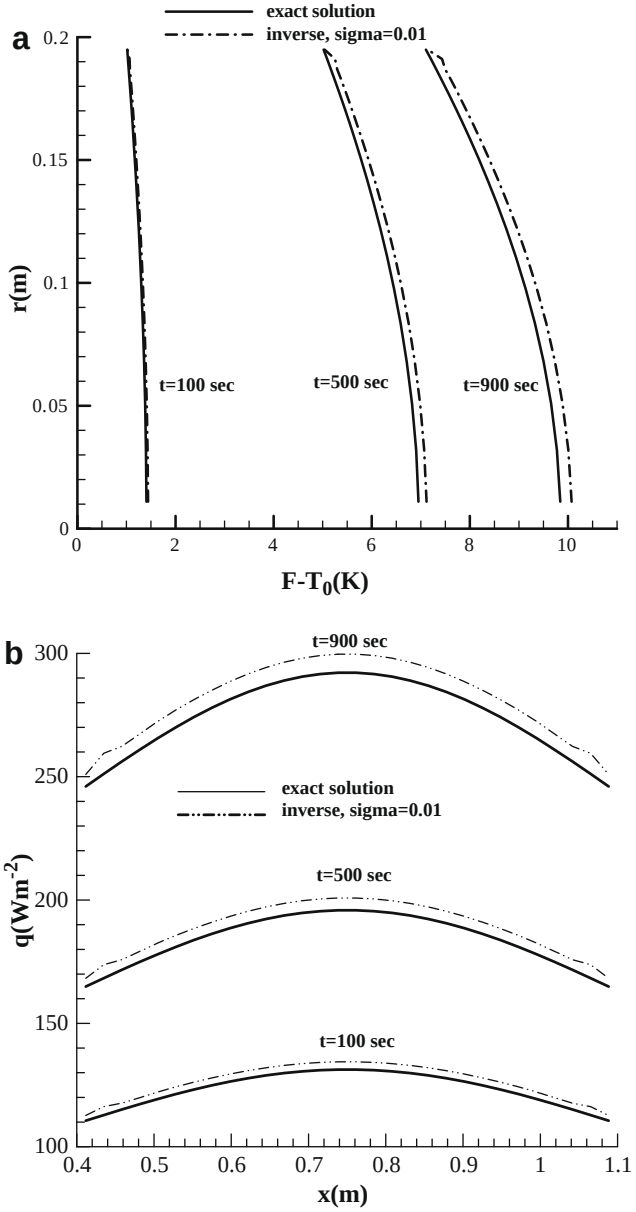

Fig. 7. Estimated distributions at $t = 100$, 500, and 900 sec, respectively, with $\sigma = 0.01$ and initial guesses $\widetilde{F}^0 = T_0$ and $\tilde{q}^0 = 0$: (a) inlet temperature $F(r,t) - T_0$ and (b) heat-transfer rate $q(x,t)$.

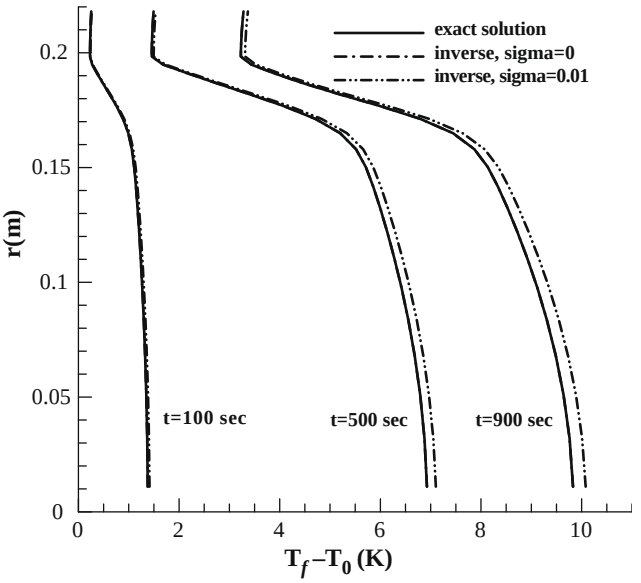

Fig. 8. Estimated temperature distributions along radial direction at $x = 0.75$ m at $t = 100$, 500, and 900 sec, respectively, with initial guesses $\widetilde{F}^0 = T_0$ and $\tilde{q}^0 = 0$, and $\sigma = 0.0$ and 0.01, respectively.

4. Conclusion

An inverse algorithm based on the conjugate gradient method and the discrepancy principle was successfully applied for the solution of the inverse problem to simultaneously determine the unknown space- and time-dependent fluid inlet temperature and heat-transfer rate on the external wall of a pipe system with the knowledge of the temperature history at some measurement locations. Subsequently, the temperature distributions in the system can be calculated. Numerical results confirm that the proposed method can accurately estimate the space- and time-dependent inlet temperature, heat-transfer rate, and temperature distributions for the problem even involving the inevitable measurement errors. In addition, the conjugate gradient method does not require prior information for the functional form of the unknown quantities to perform the inverse calculation, and excellent estimated values can be obtained for the considered problem.

Acknowledgements

This work was supported by the National Science Council, Taiwan, Republic of China, under Grant Nos. NSC 95-2221-E-168-025 and NSC 95-2221-E-168-033.

References

[1] M. Faghri, E.M. Sparrow, Simultaneous wall and fluid axial conduction in laminar pipe-flow heat transfer, ASME J. Heat Transfer 102 (1980) 58–63.
[2] E.K. Zariffeh, H.M. Soliman, A.C. Trupp, The combined effects of wall and fluid axial conduction on laminar heat transfer in circular tubes, Proc. 7th Int. Heat Transfer Conf., Munich, Germany 4 (1982) 131–136.
[3] A. Campo, C. Schuler, Heat transfer in laminar flow through circular tubes accounting for two-dimensional wall conduction, Int. J. Heat Mass Transfer 31 (1988) 2251–2259.

[4] M.A. Bernier, B.R. Baliga, Conjugate conduction and laminar mixed convection in vertical pipes for upward flow and uniform wall heat flux, Numer. Heat Transfer A 21 (1992) 313–332.
[5] Y. Jarny, M.N. Ozisik, J.B. Bardon, A general optimization method using an adjoint equation for solving multidimensional inverse heat conduction, Int. J. Heat Mass Transfer 34 (1991) 2911–2919.
[6] H.M. Park, O.Y. Chung, J.H. Lee, On the solution of inverse heat transfer problem using the Karhunen-Loeve Galerkin method, Int. J. Heat Mass Transfer 42 (1999) 127–142.
[7] H.M. Park, O.Y. Chung, An inverse natural convection problem of estimating the strength of a heat source, Int. J. Heat Mass Transfer 42 (1999) 4259–4273.
[8] M. Prud'homme, S. Jasmin, Determination of a heat source in porous medium with convective mass diffusion by an inverse method, Int. J. Heat Mass Transfer 46 (2003) 2065–2075.
[9] Y.C. Yang, S.S. Chu, W.J. Chang, Thermally-induced optical effects in optical fibers by inverse methodology, J. Appl. Phys. 95 (2004) 5159–5165.
[10] Y.K. Hong, S.W. Baek, Inverse analysis for estimating the unsteady inlet temperature distribution for two-phase laminar flow in a channel, Int. J. Heat Mass Transfer 49 (2006) 1137–1147.
[11] W.L. Chen, Y.C. Yang, H.L. Lee, Inverse problem in determining convection heat transfer coefficient of an annular fin, Energy Convers. Manage. 48 (2007) 1081–1088.
[12] C.K. Chen, L.W. Wu, Y.T. Yag, Estimation of time-varying inlet temperature and heat flux in turbulent circular pipe flow, ASME J. Heat Transfer 128 (2006) 44–52.
[13] J. Zueco, F. Alhama, Simultaneous inverse determination of temperature-dependent thermophysical properties in fluids using the network simulation method, Int. J. Heat Mass Transfer 50 (2007) 3234–3243.
[14] R.M. Hestenes, E. Stiefel, Methods of conjugate gradients for solving linear systems, J. Res. Natl. Bur. Stand. 49 (1952) 409–436.
[15] O.M. Alifanov, Determination of heat loads from a solution of the nonlinear inverse problem, High Temperature 15 (1977) 498–504.
[16] O.M. Alifanov, N.V. Kerov, Determination of external thermal load parameters by solving the two-dimensional inverse heat conduction problem, J. Eng. Phys. 41 (1981) 581–586.
[17] O.M. Alifanov, Inverse Heat Transfer Problem, Springer-Verlag, New York, 1994.
[18] O.M. Alifanov, E.A. Artyukhin, S.V. Rumyantsev, Extreme Methods for Solving Ill-Posed Problems with Applications to Inverse Heat Transfer Problems, Begell House, New York–Wallingford (UK), 1995.
[19] W.J. Chang, T.F. Fang, An inverse method for determining the interaction force between the probe and sample using scanning near-field optical microscopy, Phys. Lett. A 384 (2006) 260–265.
[20] H.L. Lee, W.J. Chang, W.L. Chen, Y.C. Yang, An inverse problem of estimating the heat source in tapered optical fibers for scanning near-field optical microscopy, Ultramicroscopy 107 (2007) 656–662.
[21] O.M. Alifanov, E.A. Artyukhin, Regularized numerical solution of nonlinear inverse heat-conduction problem, J. Eng. Phys. 29 (1975) 934–938.
[22] Y.C. Yang, Simultaneously estimating the contact heat and mass transfer coefficients in a double-layer hollow cylinder with interface resistance, Appl. Thermal Eng. 27 (2007) 501–508.
[23] O.M. Alifanov, Application of the regularization principle to the formulation of approximate solution of inverse heat conduction problem, J. Eng. Phys. 23 (1972) 1566–1571.
[24] F.S. Lien, W.L. Chen, M.A. Leschziner, A multiblock implementation of a non-orthogonal, collocated finite volume algorithm for complex turbulent flows, Int. J. Numer. Methods Fluids 23 (1996) 567–588.